Lab on a Chip

Cite this: *Lab Chip*, 2012, **12**, 1274

www.rsc.org/loc

PAPER

Single-cell recording and stimulation with a 16k micro-nail electrode array integrated on a 0.18 μm CMOS chip

Roeland Huys,†*[a] Dries Braeken,†[a] Danny Jans,[a] Andim Stassen,[a] Nadine Collaert,[a] Jan Wouters,[a] Josine Loo,[a] Simone Severi,[a] Frank Vleugels,[a] Geert Callewaert,[b] Kris Verstreken,[a] Carmen Bartic[ac] and Wolfgang Eberle[a]

Received 26th October 2011, Accepted 10th January 2012
DOI: 10.1039/c2lc21037a

To cope with the growing needs in research towards the understanding of cellular function and network dynamics, advanced micro-electrode arrays (MEAs) based on integrated complementary metal oxide semiconductor (CMOS) circuits have been increasingly reported. Although such arrays contain a large number of sensors for recording and/or stimulation, the size of the electrodes on these chips are often larger than a typical mammalian cell. Therefore, true single-cell recording and stimulation remains challenging. Single-cell resolution can be obtained by decreasing the size of the electrodes, which inherently increases the characteristic impedance and noise. Here, we present an array of 16 384 active sensors monolithically integrated on chip, realized in 0.18 μm CMOS technology for recording and stimulation of individual cells. Successful recording of electrical activity of cardiac cells with the chip, validated with intracellular whole-cell patch clamp recordings are presented, illustrating single-cell readout capability. Further, by applying a single-electrode stimulation protocol, we could pace individual cardiac cells, demonstrating single-cell addressability. This novel electrode array could help pave the way towards solving complex interactions of mammalian cellular networks.

1 Introduction

To date, the patch clamp method is the established measurement technique for the study of electrophysiological properties of cells as it allows for recording of current through single ion channels and minute changes in membrane potential.[1] However, this method has two major disadvantages. First, it is less suitable to study the behavior of large networks of cells because of its low throughput and single-cell accessibility. Second, the method is invasive, making long-term experiments hard to achieve. Therefore, micro-electrode arrays (MEAs) have been extensively employed in the last decade for the study of many electrogenic cell preparations, such as dissociated neurons, cardiomyocytes and tissue slices.[2–6] MEA's consist of a glass substrate with an array of electrodes connected to external amplifiers. So-called passive MEA systems face the disadvantage of a limited amount and density of electrodes: state-of-the-art commercial systems have up to 256 electrodes with pitches down to 30 μm.[7] The electrodes on these MEAs range from 10 to 30 μm in diameter. The disadvantage of using electrodes which are larger than the size of the cell body is that the signals of several cells are picked up: usually, local field potentials (LFP's) are recorded.[4] For detailed analysis of cellular network behavior, extensive use of signal processing algorithms such as spike sorting and principal component analysis is often required.[8] As an alternative to the glass substrates, silicon chips have been introduced by using field-effect transistors as neuron sensing devices.[9] Later, integrated circuits were developed to scale up the density and number of addressable electrodes. In such designs, the sensors were connected to an *in situ* amplifier (called "active pixel") and could be addressed either directly,[10] or by a matrix read-out scheme resulting in a higher electrode density.[11,12] A more optimized multiplexing scheme has been reported in 2009 by Frey *et al.*[13] In CMOS sensor array architectures, a trade-off has to be made between electrode density and signal-to-noise ratio (SNR). The use of larger electrodes has the advantage of increased signal strength and allows a larger area for the *in situ* circuits resulting in a better SNR, however, there are difficulties in addressing signals on a single-cell level. In contrast, the use of small sub-cellular sized electrodes allows for the design of high density arrays and, in theory, single-cell recording and stimulation, but face the difficulty of achieving signals with good SNR. True random accessibility with a single-cell resolution was, according to our knowledge, not demonstrated before.

[a]*Imec vzw, Kapeldreef 75, 3001 Leuven, Belgium. E-mail: huys@imec.be; Tel: +32 16 288942*
[b]*KULeuven, Research Group Neurodegeneration, Subfaculty Kortrijk, Katholieke Universiteit Leuven, E. Sabbelaan 53, 8500 Kortrijk, Belgium*
[c]*KULeuven, Department of Physics and Astronomy, Laboratory of Solid-State Physics and Magnetism, Katholieke Universiteit Leuven, Celestijnenlaan 200d - bus 2414, 3001 Heverlee, Belgium*
† These authors contributed equally to this work.

In previous work, we demonstrated that a passive MEA with titanium nitride electrodes (diameter 1.2 μm) allowed specific and localized stimulation of single mammalian cells.[14] In order to make the next step toward single-cell high-density addressability, we fabricated an active CMOS chip in TSMC 0.18 μm technology with custom processed micro-nail shaped electrodes. The SiO_2 micro-nails have a diameter of 1.2 μm, and contain a tungsten electrode with a diameter of 600 nm. In this paper, we demonstrate single-cell addressability for recording and stimulation in two experiments. First, we show action potential recording from an individual cardiomyocyte located directly on top of an electrode. The signals of neighboring cells could be recorded with a significant delay, caused by the dynamics of the cellular network. Second, we show that these electrodes were capable of pacing cells either directly, when the cell was on top of the stimulation electrode, or indirectly, when the cells were on neighboring electrodes. In the latter case, a time delay in activation was observed typical for communication in a cellular network. Additionally, neighboring electrodes void of cells failed to activate nearby cells.

2 Results and discussion

2.1 Chip and electrode characterization

The chip features a matrix of 16 384 units (microcells), each providing *in situ* amplification, electrical stimulation, and impedance measurement. The chip and the package are shown in Fig. 1 and a schematic overview of the circuitry is illustrated in Fig. 2.

After packaging, the chips were tested with a PCB, connected via a USB link to a PC with custom software. An Agilent 4395A network/spectrum analyzer was used to measure the analog chip functions. The different chip specifications are presented in Table 1.

The amplifier gain is digitally selectable in three ranges: 20 dB, 40 dB and 65 dB. In the highest gain setting, the average measured gain was 67.5 dB, equivalent to a factor of 2370. This setting is used in the experiments with cardiac cells described below. The amplifier has a DC offset control loop which acts as a high-pass filter with a digitally selectable cut-off frequency, ranging from 0.4–400 Hz. This circuit allows compensation of DC offset, slow drifts and low-frequency noise originating from the electrode. For the cardiac physiological experiments in this paper, a cut-off frequency of 0.4 Hz was selected to prevent the typically slow components of cardiac action potentials being filtered out. The noise of the amplifier was measured in

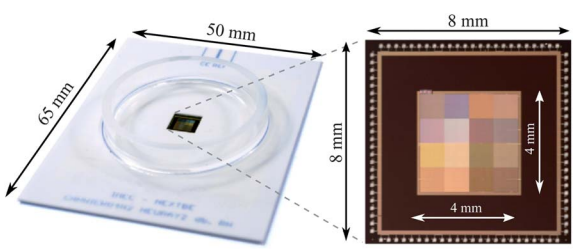

Fig. 1 Photograph of the ceramic substrate with backside flip-chip bonded chip and culture chamber, and a photograph of the die.

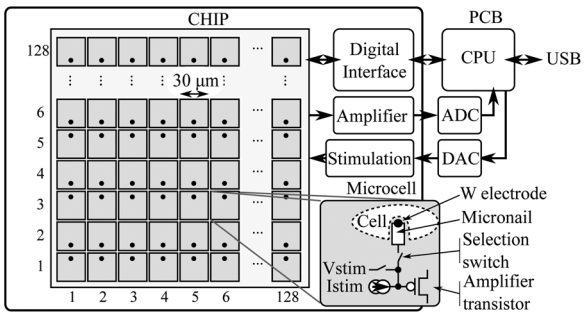

Fig. 2 Schematic representation of the chip architecture and basic printed circuit board (PCB) components. One microcell is illustrated, containing the *in situ* circuits for voltage and current stimulation, an amplification transistor, and the micro-nail electrode, connected to a cell.

a bandwidth of 0.4 Hz–5 kHz, and resulted in an input-referred noise level of 4.2 ± 1.2 μV_{RMS}.

Besides the noise of the amplifier circuitry, the small tungsten electrodes contribute significantly to the noise spectrum. The noise originates mainly from the Faradaic interface.[15] Furthermore, small metal electrodes tend to have a noise spectral density with dominating lower frequencies modeled as $1/f^{\alpha}$ with $\alpha \approx 1.82$.[16] The very low-frequency noise contribution can be interpreted as electrode offset drift which can be compensated by the DC offset control loop of the amplifier. The noise of the sensor was measured in a bandwidth of 0.4 Hz–5 kHz, and resulted in an input-referred noise level of 15 ± 5 μV_{RMS}. Due to the properties of the electrode/liquid double layer, the impedance of the electrodes is expected to approximate $1/(j\omega C_{dl})^n$.[17] The impedance measurements of four tungsten electrodes tied in parallel revealed a mainly capacitive impedance ($n \approx 0.8$) with a value ranging from 6 to 9 pF. This corresponds to a characteristic electrode capacitance of 530–800 μF cm^{-2}. The large impedance variation of electrodes can be explained by the roughness and porosity of tungsten, as reported before.[18]

2.2 Recording cardiomyocyte cell layers with single-cell resolution

With commercial micro-electrode arrays, electrical activity from cultured cardiomyocyte cells is typically measured under the form of field potentials, which are the summated electrical activity from multiple cells. By using electrodes that are significantly smaller in size than the cell body, we aimed to achieve recordings that are limited to the activity of one single cell.

To measure electrical activity from an individual cell and prove recording functionality of the electrode array, we cultured embryonic cardiomyocytes for 4 days on the chips. Once adhered, these cells spread out on the surface and ensure electrical contact from one cell to the other through electrical synapses or *gap junctions*, resulting in synchronous action potentials. These action potentials were measured by the chip as follows. First, a cell was selected by optical microscopy. Then, the intracellular membrane potential was monitored using the whole-cell patch clamp method. Finally, the sensor and read-out circuitry underneath the cell was enabled, and the extracellular signals were recorded in parallel with the intracellular signals obtained by the patch-clamp amplifier. Fig. 3 shows a typical

Table 1 Chip specifications

General chip specifications	
Technology	TSMC 0.18 μm
Digital/analog core voltage	1.8 V/3.3 V
Power consumption, recording mode	35 mW
Die size	8 × 8 mm
Active area size	4 × 4 mm
Readout matrix	128 × 128 = 16 384 microcells
Sensor specifications	
Electrode area	4 × 0.283 μm^2 = 1.13 μm^2
Characteristic electrode capacitance	7.5 ± 1.5 pF
Input-referred sensor noise	15 ± 5 μV_{RMS}
Amplifier specifications	
Bandwidth	0.4 Hz–5 kHz
Gain ranges	20, 40, 60 dB
Maximum gain	67.5 ± 1.5 dB (≈ 2600)
Input-referred RMS noise of the amplifier	4.2 ± 1.2 μV_{RMS}
Stimulation circuit specifications	
Voltage stimulation range	0–3.3 V
Current stimulation range	0.1 pA–100 nA
Input resistance	>1 TΩ
Input capacitance	0.3 pF

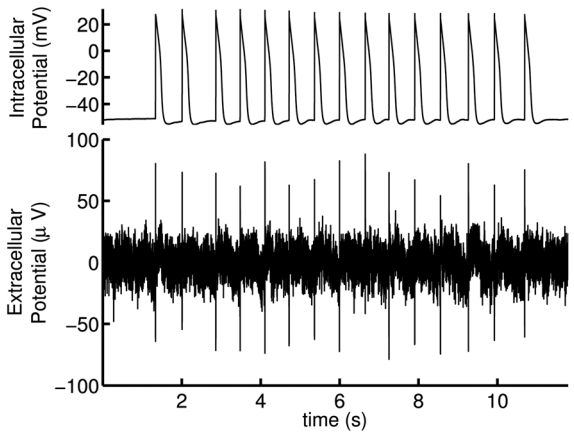

Fig. 3 (**top**) Intracellular recording of an embryonic cardiomyocyte, measured with the whole-cell patch-clamp. (**bottom**) Simultaneous extracellular recording performed by the micro-nail electrode located directly beneath the cell.

trace of the simultaneous intra and extracellular recordings of the cell on top of an electrode. The observed extracellular spikes are clearly aligned with the upstroke of the intracellular potential.

We hypothesized that if single-cell recording would be achieved, it should be possible to record the different extracellular peaks of two neighboring electrodes and measure the delay introduced by the cellular network. This was demonstrated in the following experiment. Prior to the recording, cells were loaded with Calcein green AM to ease localization of the cells, as shown in Fig. 4C. Next, an active cell on a specific electrode was patch clamped to monitor its intracellular potential. The patch pipette was filled with propidium iodide to localize the cell (Fig. 4D). As in the experiment discussed above, the intracellular signal was recorded simultaneously with the output signal of the chip amplifier from the electrode under the patched cell (electrode 1) and two different, close-by located electrodes (electrode 2 and 3) (Fig. 4A). The distances measured between selected electrode 1 and electrodes 2 and 3 were 30 and 60 μm, respectively (Fig. 4F). Different cells were located on top of electrodes 2 and 3. The amplified extracellular recordings were filtered with a second-order Butterworth low-pass filter with a cut-off frequency of 1 kHz. The signals were averaged using a spike-based synchronized averaging algorithm, thereby synchronizing the extracellular spikes on the maximum rising edge of the intracellular action potentials. The different synchronized spikes were averaged, resulting in the graph presented in Fig. 4B. In this result, all signals which were not correlated to the intracellular spikes were averaged out, while correlated signals became clearly visible.[19]

The peak positions of the averaged signals for the three electrodes show the relative onset of the extracellular spike with respect to the rising edge of the intracellular potential. A clear and significant relative time difference between the averaged peaks of the different extracellularly measured signals on the three electrodes could be observed ($p < 0.035$). This demonstrated that the measured signals originated from other cells than the cell located on electrode 1, thus confirming the hypothesis that we were able to detect extracellular signals with a single-cell resolution of 30 μm by using electrodes with a diameter of 0.6 μm.

2.3 Single-cell electrical stimulation of cardiomyocytes with micro-nail electrodes

True single-cell stimulation is hard to establish using electrodes with large diameters. Previously, it has been demonstrated in our lab that single-cell stimulation is feasible with sub-micrometre-sized electrodes on passive micro-electrode arrays.[14] In the following experiment, we repeated this protocol on the active CMOS chips, and hypothesized that if true single-cell stimulation is possible, stimulation could only be achieved if the cell is located on top of the electrode, and indirect stimulation of neighboring cells by the presence of gap junctions in the cellular network should be observable.

Embryonic cardiomyocytes were grown for 4 days *in vitro* on the chip and were pre-loaded with Calcein Green AM to enhance localization of the cells, as presented in Fig. 5C. One cell was

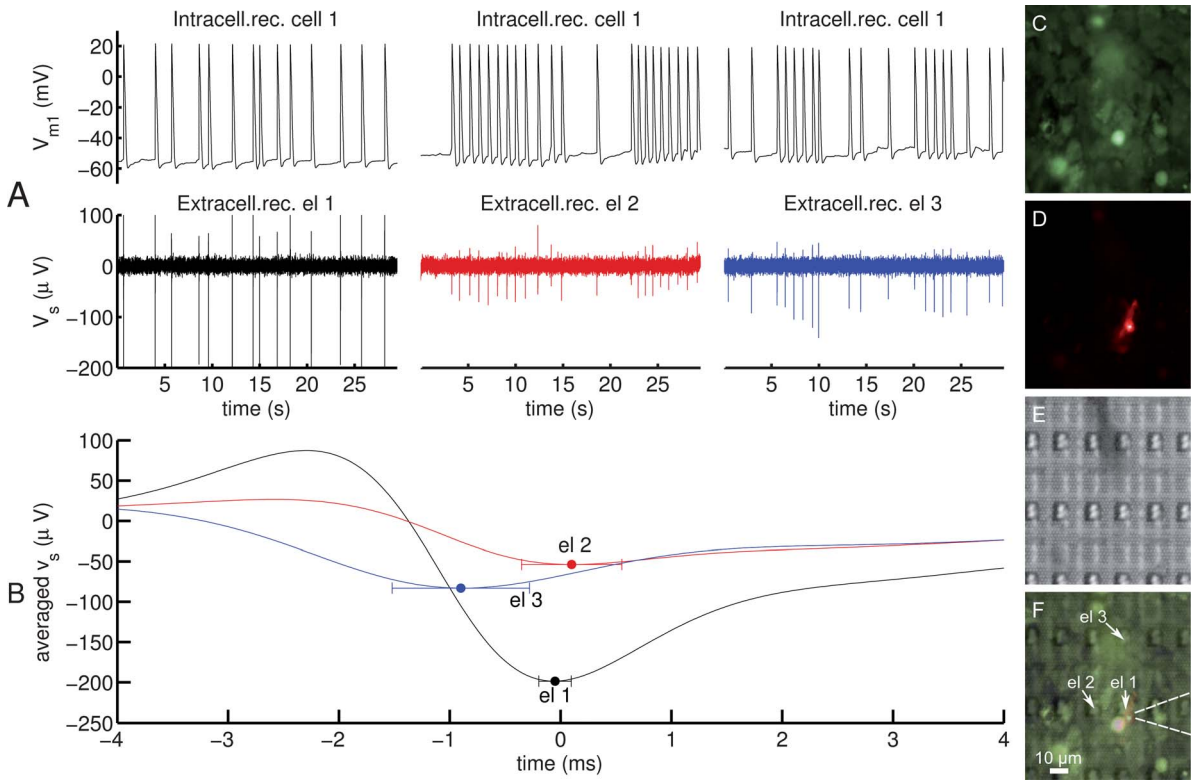

Fig. 4 (**A**) Recorded intracellular traces (V_{m1}) of the cell on top of electrode 1, combined with extracellular recordings (V_s) at different micro-nail electrodes (el 1, el 2, el 3). (**B**) Averaged extracellular signals V_s synchronized on the rising edge of intracellular signal V_{m1}. The time $t = 0$ indicates the synchronization point at the maximum of $d(V_{m1})/dt$. The error bars on the time are located on the averaged peak time offsets ($\overline{\Delta_t}$), and have a width equal to the standard deviation of the peak times (σ_t). The values for electrode 1 were: $\overline{\Delta_{t1}} = -50$ µs, $\sigma_{t1} = 146$ µs, electrode 2: $\overline{\Delta_{t2}} = -100$ µs, $\sigma_{t2} = 452$ µs, electrode 3: $\overline{\Delta_{t3}} = -850$ µs, $\sigma_{t3} = 640$ µs. The average time offsets between electrodes 1 and 2 ($\overline{\Delta_{t2}} - \overline{\Delta_{t1}}$), and 1 and 3 ($\overline{\Delta_{t3}} - \overline{\Delta_{t1}}$) were significantly different, $p_{12} = 0.037$ and $p_{13} = 1.2 \times 10^{-6}$, using two-sample unpaired t-tests. (**C**) Fluorescent image of the cardiomyocytes loaded with Calcein green AM. (**D**) Patched cell loaded with propidium iodide (red). (**E**) Brightfield image of the chip surface. (**F**) Overlay image of C, D and E. The dotted lines represent the patch pipette recording from cell 1.

patched using the whole-cell patch-clamp method. The patch pipette was filled with propidium iodide to indicate the location of this cell, as shown in panel D in Fig. 5. Underneath this cell, an electrode was located, which will be referred to as electrode 1. This cell was digitally selected with the CMOS circuits, and a biphasic rectangular voltage pulse (amplitude: 1.8 V, width: 130 ms, frequency: 0.67 Hz) was applied while recording the intracellular potential. This stimulation protocol was repeated on different electrodes: electrodes 2 and 3 were located 30 µm from electrode 1 to the left and right respectively, each with different cardiac cells on top. Electrode 4 was located 60 µm from electrode 1 and had no cell on top. The configuration of the electrodes is shown in Fig. 5F. While these stimulation protocols were applied, the intracellular potential of the cardiac cell located on top of electrode 1 was recorded. These four different traces were then visualized together, aligned on the rising flanks of the stimulation pulses. This result is shown in panel A, and allowed comparison of the effects on the same cell while using different stimulation electrodes. A detailed zoom of the effect of a single stimulation pulse is presented in panel B in Fig. 5. Labels (a) and (b) represent the stimulation artifacts. Stimulation with electrodes 1, 2 and 3 resulted in evoked action potentials and synchronized pacing of the cardiac cell. In all three cases, a downward stimulation artifact and hyperpolarization (a) was observed at the falling edges of the pulses due to the electrical field spreading. For electrode 1 (located underneath the cell), this artifact was larger than for the other electrodes. Also, the action potentials were evoked shortly after the rising edge of the stimulation pulse (b) for electrode 1, while stimulating electrodes 2 and 3 resulted in indirectly evoked action potentials with a significant delay (c) or sometimes no effect if the depolarizing threshold potential of the cell was not reached (d). Stimulation applied with electrode 4 did not result in generation of action potentials; the spontaneous pacing of the cell at a frequency of 0.25 Hz was recorded. Here, no stimulation artifacts could be observed. This result can be explained as follows. If a cell was located directly on top of a stimulation electrode, the falling edge of the stimulation pulse resulted in a direct capacitive hyperpolarization, while the rising edge resulted in a direct depolarization of the intracellular potential over the threshold potential, resulting in fast opening of the Na^+ channels of the cell and an evoked action potential. Due to the small size and confinement of the electrical field of the electrodes, this effect was not observable for neighboring cells which were not located directly on top of the electrode. The observed delay due to indirect stimulation of the neighboring cells can be explained by the presence of gap junctions.

From this experiment we can conclude that single-cell addressability is conceivable with the presented electrode

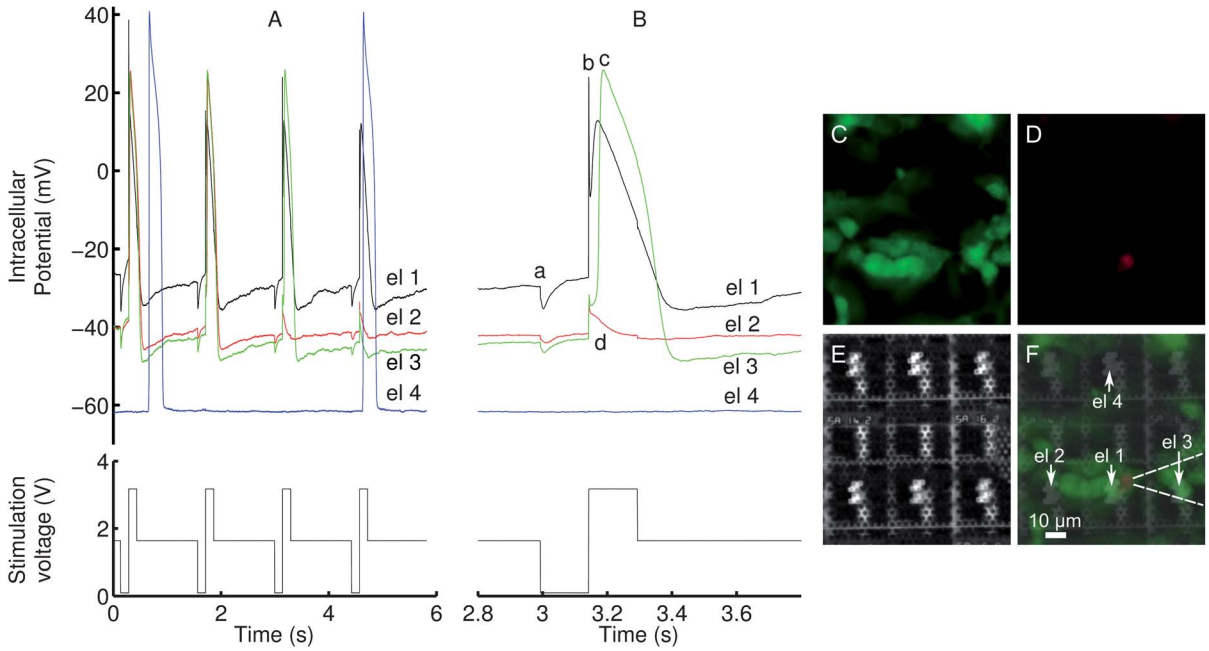

Fig. 5 (**A, top**) Intracellular recordings of an embryonic cardiomyocyte adhered to electrode 1, sequentially stimulated with electrodes 1, 2, 3 and 4. (**A, bottom**) Biphasic voltage stimuli applied on the electrodes. (**B**) Detailed trace of A, illustrating the stimulation artifacts and directly and indirectly evoked action potentials. (**C**) Photograph of the cardiac cells loaded with Calcein green AM. (**D**) Patched cardiac cell loaded with propidium iodide (red). (**E**) Brightfield image of the chip surface. (**F**) Overlay image of C, D and E. The dotted lines represent the patch pipette.

configuration. Direct stimulation is only realized when the cell is located on top of the stimulation electrode. Indirect stimulation with a delay, introduced by the cellular network, is possible by stimulating neighboring cells. Finally, bare non-covered electrodes fail to stimulate neighboring cells. These findings confirmed the hypothesis of single-cell stimulation.

3 Experimental

3.1 Chip design

The CMOS chip was designed in TSMC 0.18 µm technology. The large active area measuring 4 by 4 mm consists of 128 × 128 addressable units called microcells. Each microcell measures 30 by 30 µm and contains a local circuit and matrix of micro-electrodes. The circuit of each microcell is connected to one active electrode. The chip also contains a digital interface providing control of the on-chip functions, an amplifier circuit, a stimulation circuit for voltage and current stimulation, and circuits for other features such as calibration, testing and monitoring. The chip is bonded on a ceramic substrate and a glass ring is glued on top forming a culture chamber. The chip can be easily used in a standard electrophysiological set-up.

A schematic representation of the current stimulation, microcells, and differential amplification are shown in Fig. 2. The amplifier circuit is based on a folded cascode architecture, comprising double differential inputs (main and aux). The amplifier is capable of operating in single-ended or in differential mode. In single-ended mode, the signal of one electrode is amplified, using an external reference electrode as a virtual ground. In differential mode, the signals of two electrodes are subtracted and amplified (not demonstrated in this paper). The amplifier's main input transistors, which have the largest contribution to the noise, are located inside the microcells, thus the amplifier has virtual "remote" input transistors located in the randomly addressable matrix. The main input transistors measure 30 by 15 µm, consuming 50% of the area of one microcell. This main input transistor can be used both as a matrix selection switch as well as the amplifier transistor. The main input of the amplifier works in open-loop mode, and by altering the bias current of the main input transistors, a gain ranging from 10 to 2600 can be digitally selected. In order to cope with the low-frequency noise and DC offsets, a feedback loop is provided, using the aux input of the amplifier. This feedback loop contains an operational transconductance amplifier (OTA) with a digitally selectable bias current which forms, in combination with a capacitor, a low-pass filter. By altering the bias currents in the OTA, the cut-off frequency can be selected digitally. The chip also contains stimulation circuitry, usable for both voltage and current stimulation through the micro-electrode. Current stimulation is provided by the *in situ* PMOS and NMOS current sources (iHP and iLP), delivering currents from 1 pA to 100 nA. Cascode transistors guarantee an output DC resistivity larger than 100GΩ.

3.2 Micro-nail electrode fabrication

The chips were fabricated using 0.18 µm mixed-signal technology of TSMC with 4 metal levels. Custom micro-nail-shaped sensors with sizes ranging from 1.2 to 4.2 µm on top of the CMOS wafers were processed in the Imec 200 mm cleanroom. Briefly, the post-processing can be described as follows. On top of metal 4 (M4) of the CMOS circuits, layers of 50 nm SiC and 1.6 µm high-density plasma (HDP) SiO_2 were successively deposited. The surface was

planarized by chemical mechanical polishing (CMP) of the oxide. Another layer of 2.6 μm HDP oxide was deposited to result in a final thickness of 3 μm oxide on top of M4. A resist with a thickness of 1.8 m was spun and patterned with 600 nm holes aligned on M4 using 365 nm i-line lithography. Deep vias (3 μm) were etched down to M4, and were filled with 15 nm TaN, 15 nm Ti, 10 nm TiN, 400 nm tungsten (W) with a prolonged soft sputter etch before the TaN deposition to remove any native oxide. The W slack was removed with another CMP step, resulting in a flat surface with W-filled vias. To create the micro-nail structure, a resist pattern of 1.2–4.2 μm dots centered on the W plugs was created with i-line lithography, and plasma etching of the oxide was performed. After opening up the bondpad areas, the chips were packaged. A schematic cross-section and scanning electron microscopy (SEM) image of the processed micro-electrodes is illustrated in Fig. 6A and B, respectively. A three-dimensional reconstruction of a confocal Z-stack of cardiomyocytes growing on top of the micro-nail chip is shown in Fig. 6C.

3.3 Packaging and measurement set-up

The chips were flip-chipped using an ultrasonic bonding process at 150 °C on 600 μm-thick alumina–ceramic substrates with Ag/Pt contacts. A test PCB was developed containing a micro-controller with on-chip USB 2.0 interface, analog I/O, 8-channel 16-bit analog-to-digital and digital-to-analog convertors, and a field-programmable gate array to provide on-board control and digital signal processing algorithms. The PCB was mounted in a mechanical holder which was fixed on an upright microscope. The PCB was provided with an array of gold spring contacts to connect to the ceramic substrate and the chip, allowing easy operation with zero-insertion force.

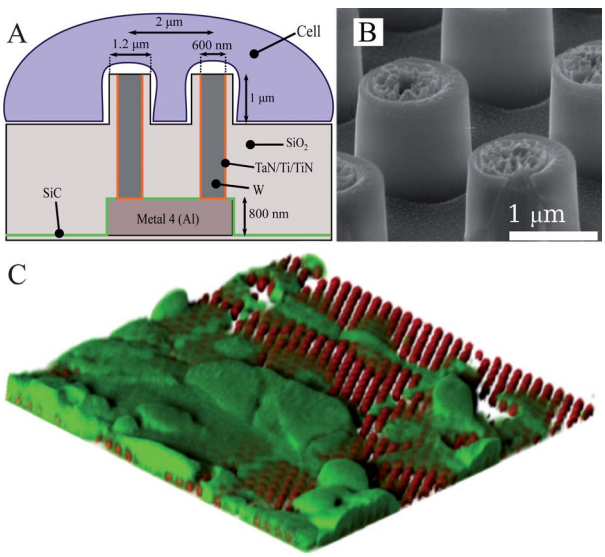

Fig. 6 (**A**) Cross-section of the micro-nail electrodes, with SiO_2 passivation, M4, and W conductor. (**B**) SEM image of the electrodes. (**C**) Three-dimensional reconstruction of confocal Z-stack of cardiomyocytes on the chip surface. Cells (loaded with Calcein green AM) were pseudo-colored in green and the micro-nail electrodes in red.

3.4 Cardiac cell cultures

Pregnant female Wistar rats (E16) were euthanized by carbon dioxide inhalation. Available embryos were removed under sterile conditions and transferred to a Ca^{2+}- and Mg^{2+}-free Hank's balanced salt solution. The ventricles of the dissected rat embryonic hearts were chopped in small fragments and collected in a Falcon tube. Enzymatic digestion was initialized in a 5 mL trypsin–ethylenediaminetetraacetic (EDTA) (0.05%) solution for 8 min at 37 °C. After removal of the supernatant, free DNA from the heart pieces was digested in the presence of 100 μL DNAse type II (10 000 units mL^{-1}, Sigma) for 3 min at room temperature. Consequently, the heart fragments passed six cycles of trypsin–EDTA treatment at 37 °C, each one lasting 8 min. After every treatment, the supernatant was recovered in 4 mL cardiac culture medium, enriched with 33% fetal calf serum (FCS, Gibco) and kept on ice. Next, the collected cells in the six tubes were centrifuged at 200*g* for 10 min at 4 °C. The cell pellets were resuspended in Hams F10 cardiac culture medium, enriched with 5% FCS, 0.5% mixture of insulin, transferrin and selenite and 0.1% penicillin/streptomycin and plated for 90 min in small dishes for selective adhesion of cardiac fibroblasts. Subsequently, the cells in the solutions on top were recollected and centrifuged at 200*g* for 10 min at 22 °C. The cell pellets were resuspended in 1 mL of cardiac culture medium and counted. Cells were seeded at a density of 100 000 cells mL^{-1} and incubated at 37 °C. Cells were used for experiments after minimally 2 days of culture and up to 6 days.

All experiments with live animals were carried out in accordance with protocols approved by the local university animal ethics committee and in accordance with the European Communities Council Directive of November 24, 1986 (86/609/EEC).

3.5 Fluorescence imaging

Cardiac cells in the stimulation experiment were pre-loaded with Calcein green AM (2 μM, excitation at 490 nm, emission at 520 nm), while the patch pipette was pre-loaded with propidium iodide (3 nM, excitation at 535 nm, emission at 617 nm) to identify the patched cell. Images were taken with an Examiner upright microscope equipped with a 20× water immersion objective (Carl Zeiss, Germany) and a DG-4 lamp from Sutter Instruments, USA. Confocal images were taken with a LSM780 confocal microscope using an argon laser at excitation wavelength 488nm and 3D-reconstruction was performed with the Zen software (Carl Zeiss).

3.6 Whole-cell patch clamp recordings

The cells were patch clamped in whole-cell configuration with pipettes pulled by the Zeitz DMZ puller (Zeitz Instruments GmbH, Martinsried, Germany) from borosilicate glass capillaries (BF150-110-10) or from quartz glass pipettes using a laser puller (P-2000, Sutter, Novato, CA, USA). The pipettes were filled with a solution that has the following composition: 140 mM KCl, 5 mM NaCl, 5 mM Na_2ATP, 10 mM HEPES, 1 mM $MgCl_2$, pH 7.2. Pipettes having a resistance in the range of 1.5 to 4.0 MΩ were used. A patch clamp amplifier (Multiclamp 700B, Axon Instruments, Molecular Devices, USA) was used in

combination with the A/D converter (Digidata 1440A, Axon Instruments, USA) and pClamp 10 software (Molecular Devices, USA) was used to acquire the patch-clamp data. Changes in membrane potential were recorded during current clamp. All experiments were performed at room temperature. The data obtained by the pClamp software were further analyzed using Origin (OriginLab Corporation, USA) and Matlab (The Mathworks, USA).

4 Conclusion

We realized a CMOS micro-electrode array consisting of 16 384 individually-addressable tungsten micro-electrodes, able to locally stimulate and record the electrical activity of cardiac cells connected in a network. Simultaneous extracellular recordings with a cell on top of the sensor and intracellular recordings using the whole-cell patch clamp method showed a clear correlation. Small but significant time delays originating from coupled cells in a network were recorded by electrodes separated with a distance of 30 μm, demonstrating the ability to measure extracellular activity with single-cell resolution. Single-cell stimulation was demonstrated by simultaneous stimulation with the electrodes on chip while monitoring changes in intracellular membrane potential. Furthermore, using whole-cell patch clamp, we measured small delays in propagation of electrical signals in a monolayer of cardiac cells. The results indicate that the chip is thus capable of addressing individual cells both for recording and stimulation. Despite high electrode impedance and small size of the *in situ* input transistors compared to earlier reported systems, the chip can detect electrical activity at a high resolution. Therefore, we believe that the presented sensor array could be a first step towards a high-throughput readout matrix with fully randomly addressable micro-electrodes with single-cell resolution.

Acknowledgements

The research leading to these results has received funding from the European Union Seventh Framework Programme (FP7/2007-2013) under grant agreement n° 215486.The authors would like to thank the support on the CMOS design by the Invomec group of Imec, and the work performed by the Process Technology group in Imec. We would like to thank Dr Olga Krylychkina of Imec for the preparation of the cardiac cell cultures.

References

1 E. Neher and B. Sakmann, *Sci. Am.*, 1992, **266**, 44–51.
2 J. Dunlop, M. Bowlby, R. Peri, D. Vasilyev and R. Arias, *Nat. Rev. Drug Discovery*, 2008, **7**, 358–368.
3 J. Fahrenbach, R. Mejia-Alvarez and K. Banach, *J. Physiol.*, 2007, **585**, 565–578.
4 J. Hescheler, M. Halbach, U. Egert, Z. J. Lu, H. Bohlen, B. K. Fleischmann and M. Reppel, *J. Electrocardiol.*, 2004, **37**, 110–116.
5 F. O. Morin, Y. Takamura and E. Tamiya, *J. Biosci. Bioeng.*, 2005, **100**, 131–143.
6 V. Pasquale, P. Massobrio, L. L. Bologna, M. Chiappalone and S. Martinoia, *Neuroscience*, 2008, **153**, 1354–1369.
7 MultichannelSystems, http://www.multichannelsystems.com, Corporate website, 2010.
8 V. Pasquale, S. Martinoia and M. Chiappalone, *J. Comput. Neurosci.*, 2010, **29**, 213–229.
9 P. Fromherz, A. Offenhausser, T. Vetter and J. Weis, *Science*, 1991, **252**, 1290–1293.
10 F. Heer, S. Hafizovic, T. Ugniwenko, U. Frey, W. Franks, E. Perriard, J. C. Perriard, A. Blau, C. Ziegler and A. Hierlemann, *Biosens. Bioelectron.*, 2007, **22**, 2546–2553.
11 L. Berdondini, K. Imfeld, A. Maccione, M. Tedesco, S. Neukom, M. Koudelka-Hep and S. Martinoia, *Lab Chip*, 2009, **9**, 2644–2651.
12 B. Eversmann, M. Jenkner, F. Hofmann, C. Paulus, R. Brederlow, B. Holzapfl, P. Fromherz, M. Merz, M. Brenner and M. Schreiter, *et al.*, *IEEE J. Solid-State Circuits*, 2003, **38**, 2306–2317.
13 U. Frey, U. Egert, F. Heer, S. Hafizovic and A. Hierlemann, *Biosens. Bioelectron.*, 2009, **24**, 2191–2198.
14 D. Braeken, R. Huys, J. Loo, C. Bartic, G. Borghs, G. Callewaert and W. Eberle, *Biosens. Bioelectron.*, 2010, **4**, 1474–1477.
15 A. Hassibi, R. Navid, R. Dutton and T. Lee, *J. Appl. Phys.*, 2004, **96**, 1074.
16 E. McAdams, J. Jossinet, R. Subramanian and R. McCauley, Engineering in Medicine and Biology Society, 2006, EMBS'06. 28th Annual International Conference of the IEEE, 2008, pp. 4594–4597.
17 N. Joye, A. Schmid and Y. Leblebici, Engineering in Medicine and Biology Society, 2008, EMBS 2008. 30th Annual International Conference of the IEEE, 2008, pp. 559–562.
18 B. Wheeler, R. Williams, B. Jeffries-Nakamura, J. Lamb, M. Loveland, C. Bankston and T. Cole, *J. Appl. Electrochem.*, 1988, **18**, 410–416.
19 R. Rangayyan, *Biomedical signal analysis*, IEEE Press, 2002.

